

Electron and Energy Transfer through Bridged Systems. 9. Toward a Priori Evaluation of the Intermetallic Coupling in Bis-metal Complexes

Jeffrey R. Reimers^{*,†} and Noel S. Hush^{†,‡}

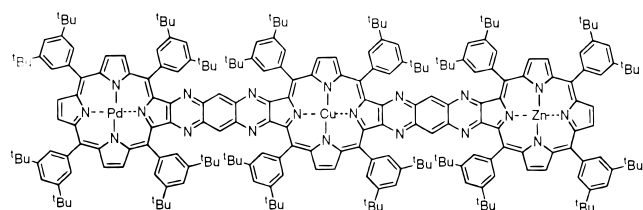
School of Chemistry and Department of Biochemistry, University of Sydney, N.S.W. 2006 Australia

Received: December 3, 1998; In Final Form: February 17, 1999

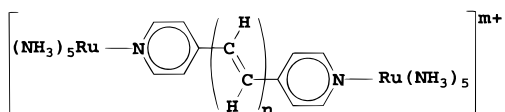
It is now commonplace to perform a priori calculations using either density functional or ab initio theory for intramolecular electron-transfer coupling strengths within organic molecules, but generally applicable a priori schemes for intermetallic couplings are yet to be determined. We examine the reasons for this, predominantly the need to treat solvent effects within the calculation, shortcomings of, or the unavailability of, Koopmans' theorem (i.e., the need for configuration interaction), and the difficulty of correctly determining ligand orbital band gaps and positioning metal orbitals within them. In particular, we model the observed intermetallic coupling in the α,ω -dipyridylpolyene-bridged ruthenium pentaammine series designed by Woitellier, Launay, and Spangler. After appropriately positioning the metal and ligand orbitals, couplings calculated using Fock matrices are found to be within 25% of experimental values. However, they attenuate too rapidly with increasing bridge length. Use of B3LYP Kohn–Sham matrices as replacements of Fock matrices yields much poorer results, however; the predicted coupling is too strong and even increases for very long bridge lengths.

Introduction

Ligand-bridged bis-metal systems such as the Creutz-Taube and related ions¹ $[(\text{NH}_3)_5\text{Ru-pyrazine-Ru}(\text{NH}_3)_5]^{m+}$ ($m = 4-6$) have been very important to the development of our understanding of through-ligand bridged intermolecular electron transfer. Their importance is set to increase further through the advent of modern molecular electronics research, in which electrode–molecule–electrode conduction is studied,² as complexes of this type can, for example, provide simple molecular models for incoherent charge-hopping through molecular wires such as



(In this³ oligoporphyrin molecular wire a graduated redox potential is achieved and the molecule appears as two diodes⁴ in series.) In particular, a very important series of electron-transfer model compounds is the symmetric α,ω -dipyridylpolyene complexes of $\text{Ru}(\text{NH}_3)_5$ designed by Woitellier, Launay, and Spangler^{5,6}



which have been synthesized for $n = 0-5$ and $m = 4-6$ (see later for full names and registry numbers). For these molecules, the intermetallic coupling has been extracted⁵⁻¹⁰ from

the transition moment of the observed intervalence charge-transfer absorption band of the $5+$ ion. The intermetallic coupling for alkane-bridged bis-ruthenium complexes is also available,¹¹ as is that for linear polyphenyl bridges.¹²

These molecules are nominally rigid with well-defined geometries covering a range of intermetallic spacings and provide quality data for the construction and verification of theories of through-molecule electron transfer (see, e.g., refs 13–15). Unfortunately, while a priori calculations for electron transfer within organic molecules are now routine, effective computational methods for inorganic complexes are still under development.¹⁶⁻¹⁸ One additional effect which must be considered is that solvent molecules interact strongly with highly charged ions, and in such these interactions are central to electron-transfer energetics. Other difficulties associated with the feasibility of large scale configuration-interaction calculations¹⁶⁻¹⁸ and difficulties in using Fock-matrix eigenvalue differences to approximate state energy differences arise in traditional ab initio approaches, while in density-functional based approaches our imprecise knowledge of the physical significance of Kohn–Sham orbital energies is a significant limitation.

So far, three approaches have been used for modeling electron transfer in the α,ω -dipyridylpolyene complexes: the empirical extended-Hückel treatment of Joachim, Launay, and Woitellier,¹⁹ our augmented self-consistent-field (SCF) approach,¹⁰ and a "CINDO/CI" approach of Sizova et al.,^{17,18} all of which yield realistic descriptions of the observed data. The Hückel treatment is important in that it shows that the intermetallic coupling is controlled by simple and well-known chemical effects. Further, approaches such as this are important to the development of the fundamental theory of electron transfer as they can yield analytical solutions¹⁵ and be readily applied in practical problems involving the modification or adaptation of well-characterized systems. The recent interesting CINDO/CI scheme of Sizova et al.^{17,18} is an a priori scheme with more advanced treatment of the electronic interactions; the quality of the results will again depend on the quality of the (possibly solvent-dependent)

[†] School of Chemistry.

[‡] School of Chemistry and Department of Biochemistry.

parametrization and are not readily subject to systematic improvement, however. In our augmented SCF approach, the ligand was treated *ab initio* but a two-parameter model was used to connect it to the solvated metal centers. The observed changes in the coupling as a function of ligand length were then directly interpreted in terms of the *ab initio* evaluated properties of the ligand. Nevertheless, this method contains significant empirical elements and is not fully satisfactory.

Effects of Solvation

The origin of the solvation effect is clarified by considering the oxidation of Fe^{2+} to form Fe^{3+} . In the gas phase, this process requires²⁰ 30.64 eV energy, but in aqueous solution it requires only 5.21 eV (the standard electrode potential is 0.77 eV with respect to the hydrogen electrode for which the absolute potential is²¹ 4.44 eV). Interpreted using Koopmans' theorem, this implies that the HOMO orbital of Fe^{2+} is raised in energy by 25.43 eV as a consequence of solvation.

While in empirical and semiempirical approaches solvent effects can be implicitly included through the parametrization, in principle the operation of such a large solvation effect suggests that no *ab initio* or density-functional calculation could be performed for a transition-metal complex unless solvation is explicitly included. In practice, gas-phase calculations on transition-metal complexes have been shown to be quite successful in a number of areas, however, and this comes about because the orbital occupation is often *not* affected, even though the orbital energy changes are large. Further, because solvation has very similar effects on all of the orbitals of the metal and hence, for example, the relative ordering of the d orbitals often remains invariant.

Indeed, the relative ordering of the orbitals is not affected by solvation of the Woitellier, Launay, and Spangler complexes. We exploit this and optimize gas-phase geometries for the ions with $m = 4$ (II–II complexes) for $n = 0, 1, 2, 3, 4,$ and 6 using the B3LYP density functional with a 3-21G basis set via Gaussian-94,²² and the resulting optimized structures are shown in Figure 1. All subsequent analyses are performed at these geometries; technical innovations necessary to complete calculations of this type on large bis-metal complexes are discussed elsewhere.²³ In these calculations, systematic overestimates of ruthenium to ammonia nitrogen bond lengths of 0.05 Å and ruthenium to pyridyl nitrogen bond lengths of 0.10 Å occur (for similar studies see, e.g., refs 24–27); while this does have some quantitative effects on metal to ligand couplings²⁶ and has large effects on properties such as d–d transition energies,²⁸ it is ligand-length independent and is not expected to affect our conclusions.

During the geometry optimizations, all molecules were constrained to C_{2h} symmetry, with the π symmetry plane bisecting pairs of equatorial ammonia ligands. Although these molecules are believed to be planar and rigid, significant conformational flexibility occurs,¹⁰ particularly for the sterically strained $n = 0$ species. Using model experimental torsional potentials, we have introduced a correction for this effect into the observed coupling strengths. Later in Table 2 where calculated and observed couplings are compared, we report both the raw observed couplings, J_{raw} , and those¹⁰ as modified for ligand flexibility, J_{corr} .

There is also a class of electronic structural properties which are significantly affected by solvation for which the solvation can be treated as a perturbation to the gas-phase property. An example of this is the metal-to-ligand charge-transfer absorption band center of ruthenium complexes,^{24,26,29} though, provided

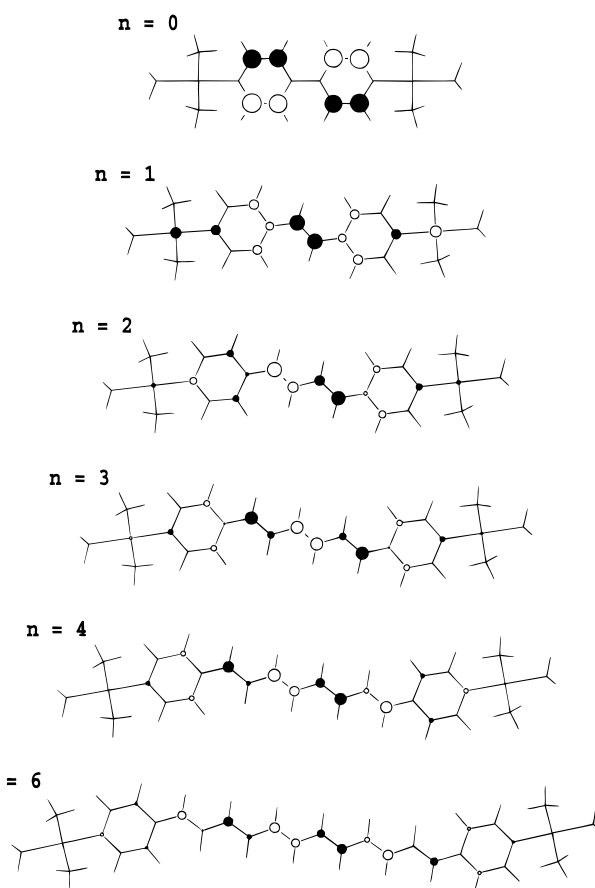


Figure 1. SCF/3-21G ligand HOMO orbitals and C_{2h} B3LYP/3-21G optimized geometries (projected onto the symmetry plane) for $[\text{Ru}(\text{NH}_3)_5\text{-}\alpha,\omega\text{-bipyridylpolyene-Ru}(\text{NH}_3)_5]^{4+}$ complexes of varying polyene chain length n . Note the increasing polyene-type character as the chain length increases.

specific solvent–solute interactions such as hydrogen bonding are not involved, such spectral properties can be evaluated directly for solvated molecules using self-consistent reaction-field (SCRf) technology.³⁰

However, a property which cannot reliably be determined from the gas-phase electronic structure is the intermetallic coupling J in extended bis-metal complexes. This is because it arises as a result of *through-bond* interactions, interactions which are very sensitive to the energy gaps between the metal and ligand orbitals.^{9,13–15,31–33} An a priori means by which these couplings could, in principle, be evaluated is via SCRf theory. This approach implicitly does retain parameters relating to the solvent dielectric response and the description of the solute's cavity within the solvent, but, particularly with the advent of the SCIPCM technique of Tomasi³⁴ in which the solvent cavity is defined based on the molecular electron density, these problems have been largely overcome.

Table 1 shows the self-consistent-field (SCF) calculated orbital energies E obtained using a 3-21G basis set for the bis-ruthenium complex of 4,4'-bipyridine ($n = 0$) for the gas phase and for aqueous solution using SCIPCM. Included therein are data for the ligand highest and second-highest occupied fragment orbital (HOMO and SHOMO), and for the three pairs of metal t_{2g} -type d orbitals (for convenience these are labeled according to their description in the full molecular C_{2h} point group). As intermetallic couplings are controlled by the energy differences between the metal and bridge orbitals, the energy differences from the ligand HOMO orbitals ΔE are also included in the

TABLE 1: SCF Orbital Energies E for $[\text{Ru}(\text{NH}_3)_5\text{-4,4'-bipyridine-Ru}(\text{NH}_3)_5]^{4+}$ and the Relative Energies ΔE from the Ligand HOMO Evaluated for the Gas Phase and for Aqueous Solution Using the SCIPCM Model,³⁴ as Well as the Orbital Solvation Energy ΔE_S ^a

orbital	symmetry	gas phase		solution		ΔE_S
		E	ΔE	E	ΔE	
d_{π}	b_g	-19.03	1.13	-8.34	1.34	10.69
d_{π}	a_u	-19.48	0.68	-8.73	0.95	10.75
$d_{z^2-x^2}$	a_g	-19.68	0.48	-8.87	0.81	10.81
$d_{z^2-x^2}$	b_u	-19.68	0.48	-8.93	0.75	10.75
d_{xy}	a_g	-19.70	0.46	-8.92	0.76	10.78
d_{xy}	b_u	-19.70	0.46	-8.98	0.70	10.72
ligand HOMO	a_u	-20.16	0	-9.68	0	10.48
ligand SHOMO	b_g	-20.32	-0.16	-9.84	-0.16	10.48

^a All energies are in eV.

table, as are the solvation energies ΔE_S evaluated as the difference of the solution and gas-phase orbital energies.

It is immediately clear that solvation has a similar effect on all orbitals considered, the average solvation energy ΔE_S being -10.68 eV with a standard deviation of just 0.12 eV or 1% of the total. Its absolute magnitude is also readily understood in terms of the Born solvation model³⁵

$$\Delta E_S = \frac{-1}{2} \frac{\epsilon - 1}{\epsilon} \frac{q_f^2 - q_i^2}{a} \quad (1)$$

for a charge change from q_i to q_f in a cavity of radius a in a dielectric medium of dielectric constant ϵ ; using the value of the radius of $a = (3V/4\pi)^{1/3} + 0.5 \text{ \AA} = 5.1 \text{ \AA}$ as recommended by Gaussian-94 where V is the volume throughout which the electron density of the molecule exceeds 0.001 au, this evaluates to $\Delta E_S = -12.1 \text{ eV}$, in good agreement with the sophisticated SCIPCM result. For the case of the oxidation of Fe^{2+} in water discussed previously, this simple treatment (using $a = 1.48 \text{ \AA}$ obtained for high-spin Fe^{3+}) predicts $\Delta E_S = -24.1 \text{ eV}$, in excellent agreement with the experimental value of -25.43 eV.

The 1% variation discussed above is systematic in nature in that the metal orbitals shift more than do the ligand orbitals, and this has a severe impact on the ligand to metal orbital energy differences ΔE which increase by 50–100% on solvation. Hence, this small variation of a large quantity becomes one of the most significant factors in determining intermetallic couplings. This is manifest in the calculated splittings between the paired metal orbitals, a very useful descriptor of the intermetallic coupling strength: in some cases, this changes by over an order of magnitude on solvation.

While SCRF-based approaches offer a way forward, they have many disadvantages. First, they dramatically increase the computation time and degrade convergence, serious problems given that the evaluation of properties of inorganic complexes such as these are inherently both computationally expensive and poorly convergent. Second, manipulation of symmetry information provides many simplifications, facilitating the evaluation of intermetallic couplings in symmetric systems. Algorithms such as SCIPCM which determine numerically the location of the solvent surface thus must construct surfaces which precisely obey the symmetry constraints, but many programs including Gaussian-94 do not do this. Finally, it must be established that SCRF approaches can faithfully reproduce the effects of differential ligand and metal solvation.

Orbital Shifting

Our aim is to find a readily applicable method for the evaluation of intermolecular couplings through molecular wires

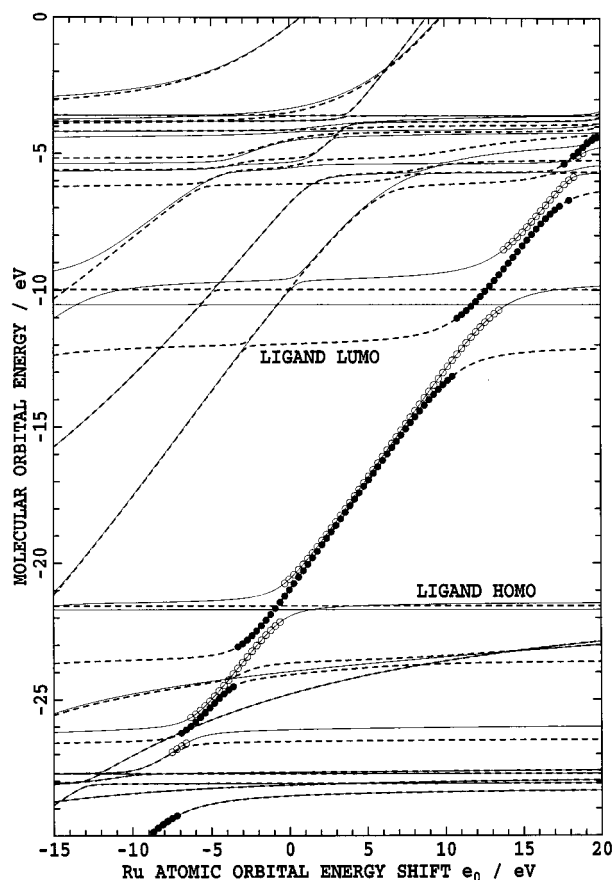


Figure 2. Orbital eigenvalues for $[\text{Ru}(\text{NH}_3)_5\text{-4,4'-bipyridine-Ru}(\text{NH}_3)_5]^{4+}$ obtained after adding the energy shift e_0 to the gas-phase orthogonalized 3-21G Fock matrix \mathbf{F} . (—) b_g orbitals, (---) a_u orbitals, (●) b_g d_{π} orbital; (O) a_u d_{π} orbital.

and switches. In this capacity we have already²³ considered oligoporphyrin systems^{3,36} connected to metals both via inner-ring complexation and via 1,10-phenanthroline linkages. These systems can be very large, e.g., bis-metal porphyrin tetramers, and so a robust an efficient computational scheme is essential. We proceed by introducing a heuristic scheme based on modification of the gas-phase orthogonalized molecular Fock matrix \mathbf{F} . To each diagonal matrix element $F_{\mu\mu}$ with μ located on one of the metal centers is added an offset energy e_0 which is intended to model the differential solvation between metal and ligand orbitals. This assumes that the solvation of each metal orbital is the same (the standard deviation in this quantity from Table 1 is 0.25 eV) as is the solvation of each ligand orbital. Simply by repetitive diagonalization of the modified Fock matrix, the entire manifold of possible solvation effects is modeled as a function of one parameter, e_0 .

Calculated π -molecular-orbital eigenvalues for $[\text{Ru}(\text{NH}_3)_5\text{-4,4'-bipyridine-Ru}(\text{NH}_3)_5]^{4+}$ as a function of the metal energy shift e_0 are shown in Figure 2. This plot consists of a set of horizontal lines (corresponding to the ligand orbitals) intersected by a set of lines of unit slope (corresponding to the metal orbitals), complicated somewhat through the presence of avoided crossings. Each avoided crossing corresponds to a resonance between metal and bridge orbitals. The molecular orbitals most reminiscent of the metal d_{π} orbitals are identified by projection onto the $e_0 = \infty$ solution and are indicated in Figure 2 by circles. When a resonance is crossed, the identity of the orbitals so selected changes. At $e_0 = 0$ (i.e., the actual SCF gas-phase result), only the metal d_{π} orbitals lie within the ligand band gap (-20 to -10 eV), although they in fact lie within the

TABLE 2: Comparison of Calculated Coupling Magnitudes J^{cen} (Two-Level Model, e_0 at Band Gap Center), J^{solv} (Two-Level Model, e_0 Given by Eqs 2 or 4), and J_n^{cen} (n -Level Model, e_0 at Band Gap Center) (in eV), the Intermetallic Separation, and the Bridge HOMO–LUMO Gap (in eV) Evaluated for the II–II Species as Well as the Observed Couplings J_{raw} and J_{corr} (See Text) for the Mixed-Valence II–III Species (in eV)

n	$R/\text{\AA}$	observed		SCF				B3LYP		
		J_{raw}	J_{corr}	J^{cen}	J^{solv}	J_n^{cen}	gap	J^{cen}	J^{solv}	gap
0	11.34	0.048	0.057	0.074	0.074	0.069	11.8	0.108	0.103	5.3
1	13.75	0.037	0.041	0.051	0.050	0.035	9.8	0.095	0.093	4.3
2	16.13	0.032	0.035	0.041	0.034	0.034	9.0	0.085	0.083	3.5
3	18.53	0.028	0.031	0.025	0.026	0.019	8.3	0.077	0.077	3.0
4	20.95	0.024	0.026	0.020	0.021	0.019	7.8	0.074	0.076	2.6
6	25.80			0.012	0.013	0.011	7.0	0.077	0.077	1.3

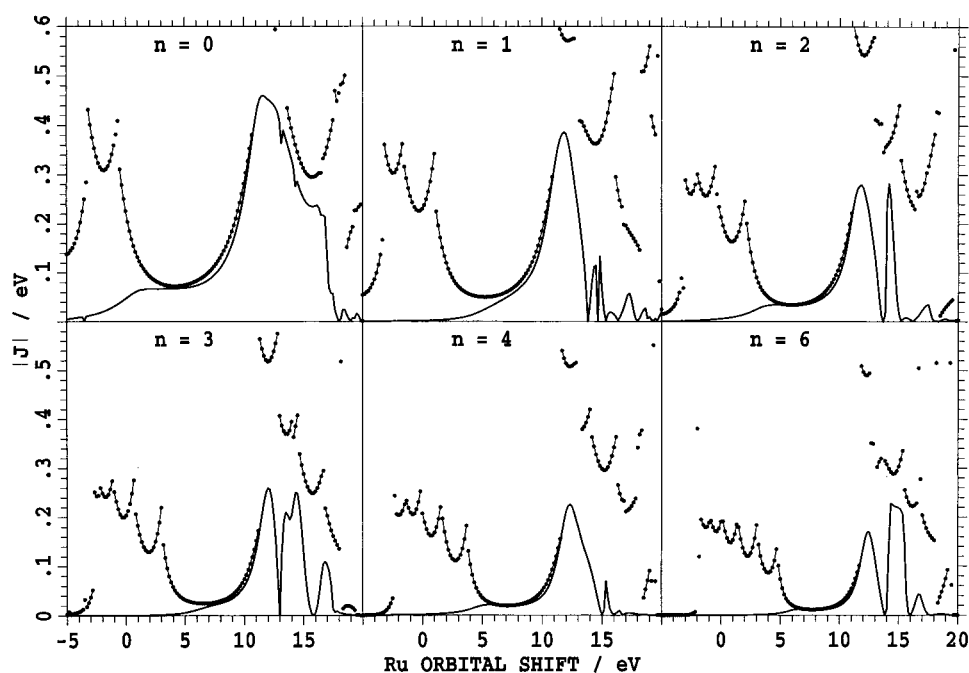


Figure 3. SCF-calculated effective two-body intermetallic d_{π} coupling J (●) and generalized electron-transfer coupling J_n (–) for bridges of length n , evaluated as a function of an imposed shift e_0 of the metal atomic orbital energies.

ligand–HOMO resonance zone. Values of e_0 so large as to take the d_{π} orbitals above the ligand LUMO (>10 eV), and values so small as to place the metal $5p$ or e_g -type $4d$ orbitals below the ligand HOMO (<-16 eV) are unphysical in that they would lead to a change in orbital occupation (corresponding to ligand reduction or oxidation) and also actually require a new Fock matrix. Nevertheless, the behavior of the system in these regions remains interesting as different behavioral patterns are exposed.

Intermetallic Coupling

Intramolecular electronic coupling is usually described in terms of an *effective two-level* model, i.e., a model which treats the system as if it were composed only of donor and acceptor orbitals (in this case the two metal d_{π} atomic orbitals) coupled with an effective coupling J . Such approaches are ubiquitous in electron-transfer modeling, however, and for hole-transfer equate $|J|$ to half of the difference between the ionization potentials arising from oxidation from the two molecular orbitals produced by the interaction. Using Koopmans' theorem, this becomes simply half of the calculated splitting between the two d_{π} molecular-orbital energies. Spectroscopic experiments on the $5+$ ions can provide a direct experimental measure of the magnitude of the effective two-level coupling J . If the charge is delocalized over both metal centers (as in the Creutz-Taube ion), then the ion has high symmetry and $2|J|$ is the energy of the lowest electronic excitation; however, if the charge localizes

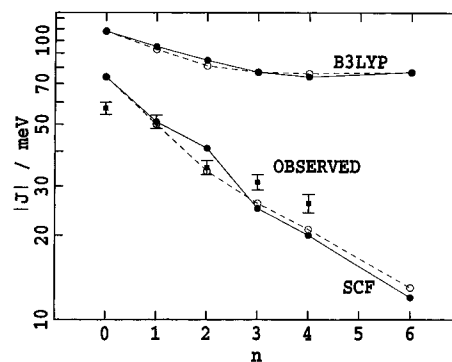


Figure 4. Observed (J_{corr} ◆, with error bars⁶) and calculated (● J^{cen} , ○ J^{solv}) intermetallic couplings on a logarithmic scale as a function of bridge length n .

to form asymmetric mixed-valence II–III species, (as is the case for the ligands considered here), then the intensity of the intervalence transition, in the absence of electron configuration interaction, scales^{7,8} proportional to J^2 . Intermetallic couplings for the α,ω -dipyridyl polyene complexes extracted in this fashion from intensity data are given in Table 2 and Figure 4 (note that this interpretation does not allow for possible configuration interaction effects). They are shown in original form as obtained from D_2O solution^{6,10} as well as with a crude correction for the likely nonplanarity of these quite flexible ligands in solution.

Couplings $|J|$, evaluated from the SCF orbital energy splitting between the two most metal- d_{π} -like orbitals, are shown as a function of the Ru orbital energy shift e_0 in Figure 3 for all complexes considered. These curves are discontinuous as, when a metal orbital crosses over a bridge orbital, the identity of the orbital with greatest metal character changes abruptly.^{14,15,23} Near discontinuities, $|J|$ becomes large due to *resonance* effects between the metal and bridge orbitals.

The SCF gas-phase calculations ($e_0 = 0$) place the d_{π} orbitals near resonance and hence a large value for $|J|$ is determined; this is a common occurrence in ab initio SCF-based calculations on ruthenium complexes.³⁷ Chemical evidence^{9,19,38,39} indicates that the d_{π} levels actually lie close to the center of the ligand band gap, however, away from resonances in a region for which the calculated coupling is much less. Unfortunately, unless very large computations involving solvent molecules are performed, we have no a priori method for determining the actual value of e_0 appropriate for any given solvent, but, given that the d_{π} levels are known to lie close to the band center^{9,30,38,40} and the insensitivity of J to e_0 in this region which is apparent from Figure 4, it would seem a reasonable assumption to select the calculated value of $|J|$ at the band center as the most appropriate calculated coupling. Such couplings J^{cen} evaluated for the complexes with $m = 4$ (II–II species) and $n = 0, 1, 2, 3, 4$, and 6 are compared to the experimental data in Table 2 and in Figure 4. We see that the evaluated couplings all fall within 25% of the observed ones, but a systematic error is apparent in that the calculated couplings are too high for short bridges and fall off at a much faster rate as bridge length n increases.

In an ab initio scheme, the accuracy of these calculations could be improved by increasing the size of the basis set, by explicitly treating solvent effects, and by explicit treatment of configuration interaction, perhaps evaluating directly the intervalence transition moment for direct comparison with the experimental data. Conceptually, two of the most significant effects of configuration interaction are to induce deviations from Koopmans' theorem and to lower electronic transition energies to ca. half of the HOMO–LUMO band gap. While our results for $n = 0$ place the metal d_{π} orbitals in the ligand HOMO–LUMO gap, as seen from Figure 3 this is not so for the longer ligands; however, explicit ionization calculations indicate that the metal is in fact preferentially oxidized with respect to the ligand, and so Koopmans' theorem provides qualitatively inaccurate results. Corrections for this effect can be made using extensive configuration-interaction calculations; while this is currently feasible using semiempirical approaches,^{17,18} it is not so ab initio. To develop a simple, improved SCF-based ab initio approach we assume that these effects are primarily responsible for the incorrect placement of the metal and ligand orbitals. Further, based on SCIPCM calculations for $n = 0$ and $n = 4$, we derive an empirical expression for the energy level shift as

$$e_0 = 5.0 + 0.3n \text{ eV} \quad (2)$$

The couplings J^{solv} evaluated using this expression are also given in Table 2; they are very similar to the couplings J evaluated simply at the center of the HOMO–LUMO band gap.

HOMO–LUMO Gap and the Bridge-Length Dependence

Often, the bridge-length dependence of the coupling is modeled using the exponential law

$$|J| = Ae^{-\alpha R} \quad (3)$$

where R is the intermetallic spacing (B3LYP/3-21G values for

R are given in Table 2). This is an example of McConnell's law,³¹ although its range of validity is in fact much wider than that as given in the original derivation.¹⁵ (Note that, because of Fermi's Golden Rule, this law is often expressed in terms of the decay of J^2 using a coefficient $\beta = 2\alpha$.) From our SCF calculations we obtain a value of $\alpha = 0.127 \text{ \AA}^{-1}$; this is very similar to the value of 0.130 \AA^{-1} obtained in our previous augmented-SCF calculations,¹⁰ indicating the robustness of the methods. However, the value extracted from the experimental data of $\alpha = 0.086 \text{ \AA}^{-1}$ is significantly smaller than these values but is reproducible using extended Hückel calculations.¹⁹ The strength of this empirical method is that while both our current and previous SCF-based approaches through Koopmans' theorem realistically describe the molecular ionization energies and electron affinities, extended-Hückel is constructed to produce much smaller HOMO–LUMO gaps consistent with observed excitation energies.³⁸ As we have demonstrated elsewhere,¹⁵ narrowing the bridge HOMO–LUMO gap results in increased resonance and decreased bridge-length attenuation.

Using Kohn–Sham Orbitals

Like extended Hückel eigenvalues, those corresponding to Kohn–Sham orbitals often have HOMO–LUMO gaps which are more consistent with excited-state energetics than are those from ab initio or semiempirical Fock matrices. It is thus interesting to consider, whether, in a heuristic approach, the Kohn–Sham matrix can be used as a replacement of the Fock matrix in intramolecular coupling calculations. For the α, ω -dipyridylpolyene complexes we thus obtained results qualitatively similar to those shown in Figures 2 and 3, and corresponding calculated couplings J^{cen} and J^{solv} are given in Table 2 using the B3LYP density functional. Indeed, the bridge HOMO–LUMO gap is much narrower (for comparison, calculated SCF and B3LYP values are given in Table 2), and, with the exception of $n = 6$, the metal d_{π} orbitals are located within it. In this case, J^{solv} is evaluated using the analogously derived equation

$$e_0 = -0.3 + 0.3n \text{ eV} \quad (4)$$

The couplings are much larger than the SCF couplings and decrease much more slowly with increasing bridge length. On average we obtain $\alpha = 0.024 \text{ \AA}^{-1}$ which is, however, now *much less* than is experimentally observed, and, at large intermetallic distances, the coupling is actually predicted to start to *increase*. This is indicative¹⁵ of a low band-gap resonance situation. Indeed, the calculated band gap of 1.3 eV for $n = 6$ is less than that observed⁴¹ for polyacetylene, 1.4 eV. As the bridge length increases, the bridge HOMO and LUMO levels become increasingly polyene-like, as indicated in Figure 1, and thus they are expected to become asymptotically more like those of polyacetylene. Further, the difference between the double and single bond lengths at the center of the $n = 6$ chain is just 0.065 \AA , less than the value of 0.07 \AA observed for polyacetylene.^{41,42} A known problem with most density-functional schemes is that they incorrectly produce no band gap in extended π systems,^{43–45} and indeed previously we have chosen B3LYP for applications such as this in the hope that it would actually produce a finite band gap³.

Electronic-State Dependence of the Coupling

A possible cause of the discrepancies found between the calculated and observed couplings is that the calculations were performed for symmetric $m = 4$ II–II ions while the experi-

mental data is obtained for the asymmetric $m = 5$ II–III ions; while analogous couplings in organic molecules are usually very similar,³ geometric and/or electronic structure variations in transition-metal complexes allow for the possibility of oxidation-state dependent coupling. It is usually believed^{30,46} that the coupling in bis-ruthenium II–II and II–III ions is quite similar, however. To test this, for $n = 0$ at the geometry of $m = 4$ we evaluated spin-unrestricted the energies of the 2B_g ground and 2A_u first excited states of the $m = 5$ symmetric ion and compared these to the orbital energy separations evaluated previously at $e_0 = 0$. At the SCF level these give $|J| = 0.180$ and 0.226 eV, respectively, while from B3LYP the results are 0.115 and 0.108 eV, respectively. This agreement is quite good and parallels that found in organic molecules,³ the greater deviation found for the SCF results being due to the bridge and metal orbital energy levels being near-degenerate and hence the coupling is very sensitive to small changes, while for B3LYP the metal orbitals lie in the middle of the bridge band gap.

Geometric Dependence of the Coupling

Also, there is the possibility that the intermetallic coupling is strongly geometry dependent: our calculations were performed at symmetric geometries for the II–II species rather than at asymmetric II–III geometries. As a partial test of this effect we optimized using B3LYP within the C_{2h} point group the structure of the $n = 0$, $m = 5$ complex; the SCF J^{cen} changed only slightly, however, from 78 to 65 meV. Calculations such as these on open-shell systems are considerably more difficult than those for the $m = 4$ ions, and at this stage it appears that our approach in using calculations on II–II ions to model properties of the II–III ions is justified.

Interference Effects

In molecular electronics applications it is more likely that the ability of the electronic coupling to facilitate long-distance electron or hole transport, rather than the ability to drive light absorption, will be of key importance. Effective two-level models are typically used to describe such processes, but in reality many coupling paths through the bridge can operate simultaneously and interference effects are possible. We have developed a comprehensive theory^{13–15} to describe this effect for the situation in which some signal (e.g., excitation, oxidation, or reduction) happens instantaneously at the donor position in a molecule, this signal then being conducted through a bridge to an acceptor from which it decays into a bath. We find that it is possible to describe the resulting kinetics in terms of an effective n -level coupling J_n which is dependent on the Hamiltonian for the system and one other parameter, a damping factor σ ¹³ which effectively sets the quantum yield for the process. The Hamiltonian can be obtained in a number of ways, representing, e.g., interactions between atomic orbitals (the Fock matrix), or interactions between electronic states (configuration-interaction matrices), etc. Here, we use the Löwdin-orthogonalized Fock matrix for the entire donor–bridge–acceptor system, or, heuristically, the Löwdin-orthogonalized Kohn–Sham matrix.

The donor and acceptor parts of the molecule are thus coupled simultaneously through all of the molecular orbitals of the bridge, and resonance and interference effects are possible. In previous calculations for electron and hole transport through ruthenium and copper oligoporphyrins,²³ we found extremely strong interference effects arising from simultaneous electron transfer through 6–10 bridge orbitals. We have repeated these calculations for the dipyridylpolyene bridges and find qualita-

tively similar results. Calculated values of J_n evaluated from the SCF Fock matrices are shown in Figure 3 and Table 2; as before,²³ we set $\sigma = 0.03$ so that the quantum yield is ca. 90%. J_n closely parallels the metal d_π orbital spacing in the bridge HOMO–LUMO gap near the LUMO side but falls to zero on the HOMO side; this reflects the chemical picture⁴⁰ that the coupling in these complexes occurs largely through the ligand LUMO. While coupling through the HOMO is strong, it is canceled by coupling through lower-lying orbitals. Note that our computation schemes evaluates (from the quantum kinetics of the original disturbance) only $|J_n|$ and, as the coupling is a signed quantity, does pass through zero due to interference effects. Sizova et al.^{17,18} have also performed calculations using this time-dependent formalism for the intermetallic coupling in these complexes implemented using CINDO methodology.

The calculated couplings obtained using the Kohn–Sham matrix pass through a minimum as the bridge length increases due to the falling band gap bringing bridge levels into resonance with the metal d_π orbitals. While this effect is clearly inappropriate for the α,ω -dipyridyl complexes of $\text{Ru}(\text{NH}_3)_5$, substituent effects can change the relative locations of the metal and bridge orbitals and hence make enhanced long-range coupling a possibility for other molecules. Previously,⁹ we have considered these effects in detail and made specific predictions. The results of this study, which indicate that the effective band gap is much narrower than the differences between the ionization energies and electron affinities, suggest that the effects described therein will in fact be considerably enhanced. The experimental synthesis and characterization of systems analogous to the α,ω -dipyridyl complexes of $\text{Ru}(\text{NH}_3)_5$ thus appears as a priority.

Conclusions

The a priori evaluation of intermetallic couplings in transition metal complexes remains a difficult computational task. We have examined the primary causes for this—how solvent effects modulate metal and ligand orbital energies, and how configuration interaction voids Koopmans' theorem to reorder electron affinities and ionization potentials and to reduce the ligand HOMO–LUMO gap. All computational schemes used to date for problems of this type have involved some empiricism; we introduced a new scheme in which empiricism remains but for which chemical and/or computational evidence can be used to determine values for the one empirical parameter. Once chosen, computations at the ab initio SCF level (or, heuristically, using the Kohn–Sham matrix in place of the Fock matrix) can then be performed for a wide range of complexes. The results presented here show that the method is readily applicable to large systems for which couplings within 25% of experimental values can be obtained. Elsewhere,²³ we have successfully applied this approach to model chemical control of intermetallic coupling through oligoporphyrin^{3,36} molecular wires, isolating the key intramolecular interactions, and hence designing new systems with improved features.

Acknowledgment. J.R.R. gratefully acknowledges support from the Australian Research Council.

Registry Numbers (supplied by the author). $n = 0$: decaammine[μ -(4,4'-bipyridine- $N:N'$)]diruthenium (4+) 36451-88-4, (5+) 54065-65-5; $n = 1$: decaammine[μ -[4,4'-(1,2-ethenediyl)-bis[pyridine]- $N:N'$]]diruthenium (4+) 78147-57-6, (5+) 77305-51-2; $n = 2$: decaammine[μ -[4,4'-(1,3-butadiene-1,4-diyl)bis[pyridine]- $N:N'$]]diruthenium (5+) 106219-83-4; $n = 3$: decaammine[μ -[4,4'-(1,3,5-hexatriene-1,6-diyl)bis[pyridine]- $N:N'$]]diruthenium (5+) 118484-83-0; $n = 4$: decaammine[μ -[4,4'-

(1,3,5,7-octatetraene-1,8-diyl)bis[pyridine-*N*:*N'*]]diruthenium (5+) 118494-84-1.

References and Notes

- Creutz, C.; Taube, H. *J. Am. Chem. Soc.* **1969**, *91*, 3988.
- Aviram, A.; Ratner, M., Eds. *Ann. N.Y. Acad. Sci.* **1998**, *852*, 1998.
- Crossley, M. J.; Johnston, L. A.; Reimers, J. R.; Hush, N. S. *J. Am. Chem. Soc.*, manuscript in preparation.
- Aviram, A.; Ratner, M. A. *Chem. Phys. Lett.* **29**, 277.
- Woitellier, S.; Launay, J. P.; Spangler, C. W. *Inorg. Chem.* **1989**, *28*, 758.
- Robou, A.-C.; Launay, J.-P.; Takahashi, K.; Nihira, T.; Tarutani, S.; Spangler, C. W. *Inorg. Chem.* **1994**, *33*, 1325.
- Hush, N. S. *Prog. Inorg. Chem.* **1967**, *8*, 391.
- Hush, N. S. *Coord. Chem. Rev.* **1985**, *64*, 135.
- Reimers, J. R.; Hush, N. S. *Inorg. Chem.* **1990**, *29*, 3686.
- Reimers, J. R.; Hush, N. S. *Inorg. Chem.* **1990**, *29*, 4510.
- Gholamkhash, B.; Nozaki, K.; Ohno, T. *J. Phys. Chem. B* **1997**, *101*, 9010.
- Hammarstroem, L.; Barigelletti, F.; Flamigni, L.; Indelli, M. T.; Armaroli, N.; Calogero, G.; Guardigli, M.; Sour, A.; Collin, J.-P.; Sauvage, J.-P. *J. Phys. Chem. A* **1997**, *101*, 9061.
- Reimers, J. R.; Hush, N. S. *Chem. Phys.* **1989**, *134*, 323.
- Reimers, J. R.; Hush, N. S. *Chem. Phys.* **1990**, *146*, 89.
- Reimers, J. R.; Hush, N. S. *J. Photochem. Photobiol. A* **1994**, *82*, 31.
- Catti, M.; Sandrone, G. *Faraday Discuss.* **1997**, *106*, 189.
- Sizova, O. V.; Panin, A. I.; Baranovskii, V. I.; Nikol'skii, A. B.; Ivanova, N. V. *Russ. J. Gen. Chem.* **1997**, *67*, 1657.
- Sizova, O. V.; Baranovskii, V. I.; Panin, A. I.; Ivanova, N. V.; Nikol'skii, A. B. *Russ. J. Gen. Chem.* **1997**, *67*, 1513.
- Joachim, C.; Launay, J. P.; Woitellier, S. *Chem. Phys.* **1990**, *147*, 131.
- Moore, C. E. *Atomic Energy Levels. Natl. Bur. Standards (U.S.) Circ.* **467**, 1958.
- Trasatti, S. *Pure Appl. Chem.* **1986**, *58*, 955.
- Frisch, M. J.; Trucks, G. W.; Schlegel, H. B.; Gill, P. M. W.; Johnson, B. G.; Robb, M. A.; Cheeseman, J. R.; Keith, T. A.; Petersson, G. A.; Montgomery, J. A.; Raghavachari, K.; Al-Laham, M. A.; Zakrzewski, V. G.; Ortiz, J. V.; Foresman, J. B.; Cioslowski, J.; Stefanov, B. B.; Nanayakkara, A.; Challacombe, M.; Peng, C. Y.; Ayala, P. A.; Chen, W.; Wong, M. W.; Andres, J. L.; Replogle, E. S.; Gomperts, R.; Martin, R. L.; Fox, D. J.; Binkley, J. S.; DeFrees, D. J.; Baker, J.; Stewart, J. J. P.; Head-Gordon, M.; Gonzalez, C.; Pople, J. A. *GAUSSIAN 94*; Gaussian Inc.: Pittsburgh, PA, 1995.
- Hush, N. S.; Reimers, J. R.; Hall, L. E.; Johnston, L. A.; Crossley, M. J. *Ann. N.Y. Acad. Sci.* **1998**, *852*, 1.
- Zeng, J.; Hush, N. S.; Reimers, J. R. *J. Phys. Chem.* **1995**, *99*, 10459.
- Zeng, J.; Hush, N. S.; Reimers, J. R. *J. Am. Chem. Soc.* **1996**, *118*, 2059.
- Zeng, J.; Hush, N. S.; Reimers, J. R. *J. Phys. Chem.* **1996**, *100*, 19292.
- Broo, A.; Lincoln, P. *Inorg. Chem.* **1997**, *36*, 2544.
- Comba, P.; Hambley, T. *Molecular modelling of inorganic systems*; VCH: Weinheim, Germany, 1995.
- Zeng, J.; Hush, N. S.; Reimers, J. R. *J. Phys. Chem.* **1996**, *100*, 9561.
- Broo, A.; Larsson, S. *Chem. Phys.* **1992**, *161*, 363.
- McConnell, H. M. *J. Chem. Phys.* **1961**, *35*, 508.
- Larsson, S. *J. Am. Chem. Soc.* **1981**, *103*, 4034.
- Joachim, C. *Chem. Phys.* **1987**, *116*, 339.
- Cossi, M.; Barone, V.; Cammi, R.; Tomasi, J. *Chem. Phys. Lett.* **1996**, *255*, 327.
- Born, M. Z. *Phys.* **1920**, *1*, 45.
- Reimers, J. R.; Hall, L. E.; Crossley, M. J.; Hush, N. S. *J. Phys. Chem.*, submitted for publication.
- Shin, Y. - K.; Brunschwig, B. S.; Creutz, C.; Newton, M. D.; Sutin, N. *J. Phys. Chem.* **1996**, *100*, 1104.
- Tatsumi, K.; Hoffmann, R. *J. Am. Chem. Soc.* **1981**, *103*, 3328.
- Zhang, L.-T.; Ondrechen, M. J. *Inorg. Chim. Acta* **1994**, *226*, 43.
- Ford, P. C.; Rudd, D. F. P.; Gaunder, R.; Taube, H. *J. Am. Chem. Soc.* **1968**, *90*, 1187.
- Su, W. P.; Schrieffer, J. R.; Heeger, A. J. *Phys. Rev. Lett.* **1979**, *42*, 1698.
- Craw, J. S.; Reimers, J. R.; Bacskay, G. B.; Wong, A. T.; Hush, N. S. *Chem. Phys.* **1992**, *167*, 77.
- Ashkenazi, J.; Picket, W. E.; Krakauer, H.; Wang, C. S.; Klein, B. M.; Chubb, S. R. *Phys. Rev. Lett.* **1989**, *62*, 2016.
- Vogl, P.; Campbell, D. K. *Phys. Rev.* **1989**, *B41*, 12797.
- Almlöf, J.; Fischer, T. H.; Gassman, P. G.; Ghosh, A.; Häser, M. *J. Phys. Chem.* **1993**, *97*, 10964.
- Zhang, L. T.; Ko, J.; Ondrechen, M. J. *J. Am. Chem. Soc.* **1987**, *109*, 1666.